

EFFECTIVE VOLT/VAR CONTROL IN LOW VOLTAGE GRIDS WITH BULK LOADS SUCH AS ELECTRIC VEHICLE GARAGES

Daniel-Leon SCHULTIS
TU Wien - Austria
daniel-leon.schultis@tuwien.ac.at

Helmut BRUCKNER
Sonnenplatz Großschönau - Austria
h.bruckner@sonnenplatz.at

Markéta ADAMCOVÁ
LEEF Technologies - Czech Republic
marketa.adamcova@leeftech.com

Markus OLOFSGÅRD
AFRY - Sweden
Markus.Olofsgard@afry.com

Andrea WERNER
FH Technikum Wien - Austria
andrea.werner@technikum-wien.at

ABSTRACT

The growing share of distributed energy resources aggravates voltage control in distribution grids. The $X(U)$ local control and its combination with Q -Autarkic customer plants are the most effective and reliable Volt/var control strategies in low voltage grids with high prosumer share. However, these strategies may need adaptations to guarantee voltage limit compliance when bulk loads such as electric vehicle parking garages are connected to the low voltage feeders. This paper extends the $X(U)$ local control concept to involve bulk loads in Volt/var control and analyzes the resulting load flows in a real low voltage grid. Results show that the extended control scheme reliably removes all voltage limit violations by increasing the reactive power flows through the low voltage feeders and distribution substations.

INTRODUCTION

The increasing share of photovoltaic (PV) systems and electric vehicle (EV) chargers challenges the operation of distribution grids [1,2]. Maintaining voltage limit compliance is a major issue for future smart grids [3]. At the same time, distributed energy resources (DER) may provide reactive power (Q) to support voltage control within the grid [4]. Local Volt/var control (VVC) schemes, such as $\cos\phi(P)$ and $Q(U)$, are well known [5], but they provoke tremendous uncontrolled reactive power flows that propagate up to the superordinate grid levels [6]. These issues are addressed by the $X(U)$ local control strategy [7] and its combination with Q -Autarkic customer plants (CP) [8], which maintain voltage limit compliance while minimizing the uncontrolled reactive power flows. The $X(U)$ concept intends the installation of variable reactive power devices (RPD), such as switchable capacitors and reactors, or power electronic-based devices, close to the ends of low voltage (LV) feeders that maintain acceptable voltages at their connection points. Meanwhile, Q -Autarkic CPs supply their reactive power demand locally and do not exchange any reactive power with the grid. However, the functioning of the $X(U)$ concept has only been validated for LV grids connecting small DERs, such as residential EV chargers and rooftop PV systems [9], but not in the presence of bulk loads.

This paper investigates the ability of the $X(U)$ local control to maintain voltage limit compliance in an LV grid that connects Q -Autarkic prosumers and bulk loads such as EV parking garages. Furthermore, the $X(U)$ local control strategy is extended to guarantee voltage limit compliance also in times of bulk consumption. The presented analysis is extended in [10] to consider bulk producers such as community-owned PV systems and different LV grids.

MATERIALS AND METHODS

This paper uses load flow analysis to evaluate the effect of different Volt/var control setups on the behavior of an LV grid connecting prosumers and an EV parking garage. This section describes the investigated control setups, the used power system model, and the procedures used to evaluate the simulation results.

Control setups

Fig. 1 shows three different VVC setups applied to an LV feeder connecting residential CPs and an EV parking garage. The setup without any VVC is shown in Fig. 1a. PV systems and EV chargers do not contribute any reactive power. Therefore, the residential CPs exchange reactive power with the LV grid to supply the demand of their household devices, such as motor-driven, lighting, and switch-mode power supply devices. Meanwhile, the parking garage does not contribute any reactive power (consuming devices such as lighting and ventilation systems are neglected). Fig. 1b shows the setup with CP- Q -Autarky and $X(U)$ local control at the feeder end, which is denoted as ' $X(U)$ & CP_{aut}^Q '. In this paper, the $X(U)$ local control bases on (lossless) power electronic devices that are capable of adjusting their reactive power contributions continuously. Q -Autarkic CPs use their PV inverter or other reactive power sources to supply the Q -demand of their household devices locally: they do not exchange any reactive power with the LV grid. $X(U)$ local control is implemented in an RPD connected at the feeder end, which contributes the reactive power required to maintain the local voltage between 0.91 and 1.09 p.u. This setup is extended in Fig. 1c, where the $X(U)$ local control is additionally implemented at the parking garage's delivery point. This control setup is denoted as ' $X(U)^+$ & CP_{aut}^Q '.

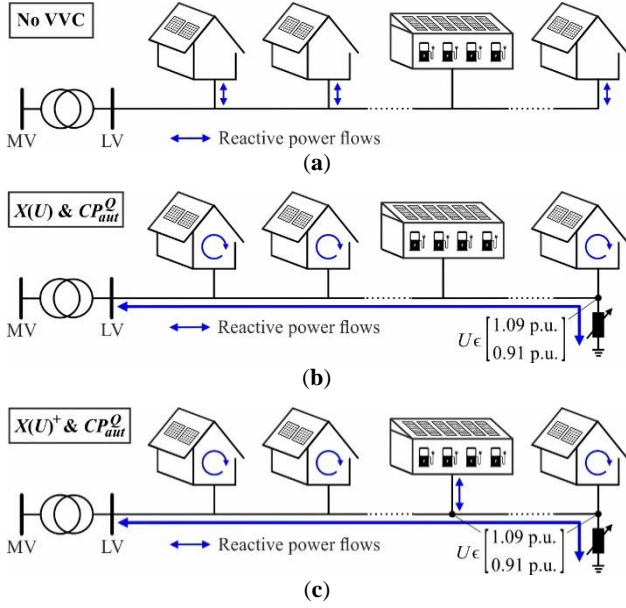


Fig. 1. Schemas of different Volt/var control setups: (a) No VVC; (b) CP_Q-Autarky and $X(U)$ local control at the feeder end; (c) CP_Q-Autarky and $X(U)$ local control at the feeder end and the parking garage's delivery point.

Power system model

The effects of the different VVC setups are investigated using load flow analysis of the low voltage level. Losses within the parking garage and CPs, as well as asymmetry, are neglected.

Residential customer plants

Fig. 2 overviews the lumped model of residential CPs. It consists of two components: a device (Dev) model representing the household devices and a producer (Pr) model representing a five kWp PV system, Fig. 2a. The active ($P_t^{LV \rightarrow CP}$) and reactive power ($Q_t^{LV \rightarrow CP}$) exchanges between the LV grid and the residential CPs at daytime t are determined by Eq. (1), wherein P_t^{Dev} and Q_t^{Dev} are the Dev.-model's actual active and reactive power absorptions, and P_t^{Pr} is the Pr.-model's active power injection. The simplified modeling of CP_Q-Autarky according to Eq. (1b) is valid as the losses at the CP level are neglected, and the corresponding reactive power source is assumed to be sufficiently dimensioned.

$$P_t^{LV \rightarrow CP} = P_t^{Dev} - P_t^{Pr} \quad (1a)$$

$$Q_t^{LV \rightarrow CP} = \begin{cases} Q_t^{Dev}, & \text{without CP}_Q\text{-Autarky} \\ 0, & \text{with CP}_Q\text{-Autarky} \end{cases} \quad (1b)$$

Fig. 2b exemplifies the load profiles specifying the power contributions of both model components at the nominal voltage (U_{nom}). The load profile generator [11] is used to synthesize individual consumption profiles for the Dev.-model of each residential CP. The Dev.-model's actual power consumption depends on the local voltage (U_t) and is determined by the polynomial load model [12] given in Eq. (2).

$$\frac{P_t^{Dev}}{P_{nom,t}^{Dev}} = 0.96 \cdot \left(\frac{U_t}{U_{nom}}\right)^2 - 1.17 \cdot \left(\frac{U_t}{U_{nom}}\right) + 1.21 \quad (2a)$$

$$\frac{Q_t^{Dev}}{Q_{nom,t}^{Dev}} = 6.28 \cdot \left(\frac{U_t}{U_{nom}}\right)^2 - 10.16 \cdot \left(\frac{U_t}{U_{nom}}\right) + 4.88 \quad (2b)$$

Where $P_{nom,t}^{Dev}$ and $Q_{nom,t}^{Dev}$ are the Dev.-model's active and reactive power absorptions at the nominal voltage. Meanwhile, the same PV production profile, generated with [13], is used for the Pr.-model of all CPs. The PV systems' active power injections are modeled voltage-independent [14].

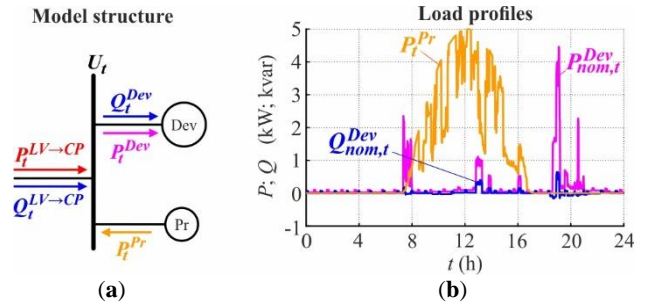


Fig. 2. Lumped model of the residential CPs: (a) structure; (b) load profiles.

Electric vehicle parking garage

Fig. 3 overviews the lumped model of the EV parking garage. It includes a storage (St) model representing the EV batteries connected through the chargers, and a Pr.-model representing a 35 kWp PV system, Fig. 3a. The active ($P_t^{LV \rightarrow EV}$) and reactive power ($Q_t^{LV \rightarrow EV}$) exchanges between the LV grid and the garage are determined by Eq. (3).

$$P_t^{LV \rightarrow EV} = P_t^{St} - P_t^{Pr} \quad (3a)$$

$$Q_t^{LV \rightarrow EV} = Q_t^{St} \quad (3b)$$

Where P_t^{St} and Q_t^{St} are the St.-model's active and reactive power contributions. Fig. 3b shows the load profiles specifying the active power contributions of both model components at nominal voltage. Four 43 kW quick chargers are active between 13:54 and 14:12, absorbing 172 kW in total. However, the St.-model's actual active power absorption depends on the local voltage and is determined by the load model [15] given in Eq. (4). The St.-model contributes reactive power to maintain the local voltage within the limits only when $X(U)$ local control is applied at the garage's delivery point (see Fig. 1c).

$$\frac{P_t^{St}}{P_{nom,t}^{St}} = -0.02 \cdot \left(\frac{U_t}{U_{nom}}\right)^2 + 0.03 \cdot \left(\frac{U_t}{U_{nom}}\right) + 0.99 \quad (4)$$

The Pr.-model's active power injection is modeled voltage-independent and follows the same pathway as the one shown in Fig. 2b (multiplied by the factor of 7).

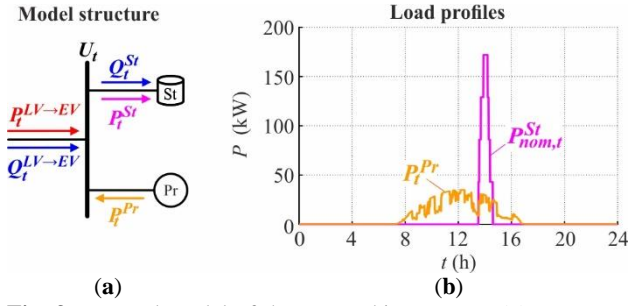


Fig. 3. Lumped model of the EV parking garage: (a) structure; (b) load profiles.

Low voltage grid

Fig. 4 sketches the real Austrian LV grid used for the simulations; its exact model data is provided in [16]. While grey crosses mark the connection points of $X(U)$ controlled RPDs, a red dot highlights the delivery point of the parking garage. The LV grid connects 175 residential CPs, includes nine feeders with a total length of 12.82 km, and has a cable share of around 96%. Its distribution transformer (DTR) has a fixed tap changer, transforms 20 kV into 0.4 kV, and is rated by 800 kVA (due to the high PV share, the 800 kVA DTR is used instead of the 630 kVA one documented in the data repository).

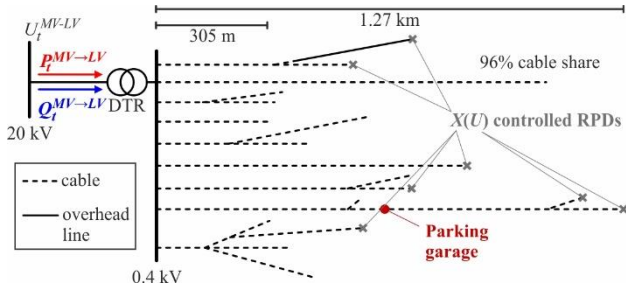


Fig. 4. Simplified one-line diagram of the LV grid model.

Result evaluation

The effects of the different VVC setups on the behavior of the LV grid are evaluated based on the voltages, reactive power flows, and equipment loadings. Voltage limit compliance is assessed by analyzing the maximal (U_t^{max}) and minimal node voltages (U_t^{min}) according to Equation (5), wherein $U_{t,n}$ is the voltage of node n .

$$U_t^{max} = \max_n(U_{t,n}) \quad (5a)$$

$$U_t^{min} = \min_n(U_{t,n}) \quad (5b)$$

The grid's reactive power behavior is analyzed based on:

- The reactive power flowing into the DTR ($Q_t^{MV \rightarrow LV}$).
- The reactive power contributed by the parking garage ($Q_t^{LV \rightarrow EV}$).
- The total reactive power contributions of all $X(U)$ controlled RPDs connected at the feeder ends ($Q_t^{LV \rightarrow RPD,E}$), calculated according to Eq. (6a).
- The total reactive power contributions of all residential CPs, calculated according to Eq. (6b).

$$Q_t^{LV \rightarrow RPD,E} = \sum_{\forall f} Q_{f,t}^{LV \rightarrow RPD} \quad (6a)$$

$$Q_t^{LV \rightarrow CP,E} = \sum_{\forall i} Q_{i,t}^{LV \rightarrow CP} \quad (6b)$$

Where $Q_{f,t}^{LV \rightarrow RPD}$ is the reactive power flowing from the LV grid into the RPD connected at the feeder end f ; and $Q_{i,t}^{LV \rightarrow CP}$ is the reactive power flowing from the LV grid into the customer plant i . Furthermore, the grid state, including voltage profiles and equipment loadings, is discussed for two critical cases that provoke high and low voltages at the LV level:

- **Case A** threatens the upper voltage limit due to high active power production ($t_1 = 12:12$) and high DTR primary voltage ($U_t^{MV-LV} = 1.04$ p.u.).
- **Case B** threatens the lower voltage limit due to high active power consumption ($t_2 = 14:06$) and low DTR primary voltage ($U_t^{MV-LV} = 0.96$ p.u.).

VOLT/VAR BEHAVIOR OF LV GRID

Voltages

Fig. 5 shows the maximal and minimal values of the LV grid's node voltages over the day. Most of the time, the VVC setups including $X(U)$ and $X(U)^+$ local control behave similarly, so the corresponding curves overlap. Meanwhile, the CP_QuAutarky modifies the grid voltages during the whole day. According to Fig. 5a, the upper voltage limit is violated many times between 9:05 and 14:53 without any VVC. Both VVC setups successfully eliminate these limit violations. Meanwhile, the lower voltage limit violations are removed only by the ' $X(U)^+$ & CP_QuAut' control setup, i.e., when the parking garage contributes reactive power, Fig. 5b.

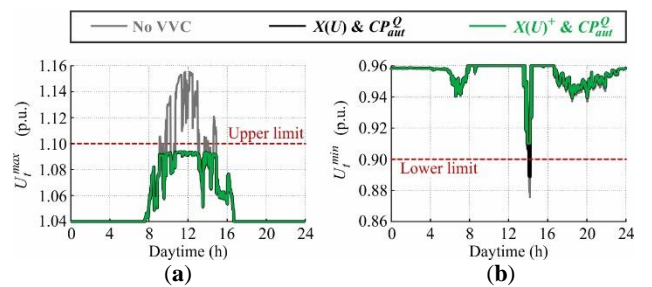


Fig. 5. Different extremums of node voltages for the investigated control setups over daytime: (a) maxima; (b) minima.

Reactive power flows

Fig. 6 shows the daily reactive power flows within the LV grid for different VVC setups and DTR primary voltages. Without any VVC, no RPDs are connected to the LV grid, and the EV parking garage does not contribute any reactive power. Therefore, only the reactive power contributions of the CPs, LV lines, and the DTR determine the Q -flows at the distribution substation level. The high reactive power flows around midday, shown in Fig. 6a and 6d, are mainly attributable to grid losses arising from the massive active

power injections of the PV systems, especially when the DTR primary voltage is set to 0.96 p.u. As Fig. 6b and 6e show, the ' $X(U) & CP_{aut}^Q$ ' control setup fundamentally modifies the system behavior: the CPs do not contribute any reactive power, so only the RPDs and grid losses determine the MV-LV reactive power exchange. When the slack voltage is set to 1.04 p.u., the RPDs consume large Q -amounts around midday to maintain acceptable voltages. Meanwhile, for a slack voltage of 0.96 p.u., the RPDs inject some reactive power to keep the voltages at the feeder ends above the lower limit.

Fig. 6c and 6f illustrate the reactive power flows resulting from the ' $X(U)^+ & CP_{aut}^Q$ ' control setup. For a DTR primary voltage of 1.04 p.u., the EV parking garage absorbs some reactive power around midday, slightly reducing the RPDs' total Q -consumption while increasing the MV-LV reactive power exchange. When the slack voltage is set to 0.96 p.u., the EV parking garage consumes large Q -amounts around 14:06 to maintain voltage limit compliance at its connection point. Here, the RPDs do not contribute any reactive power.

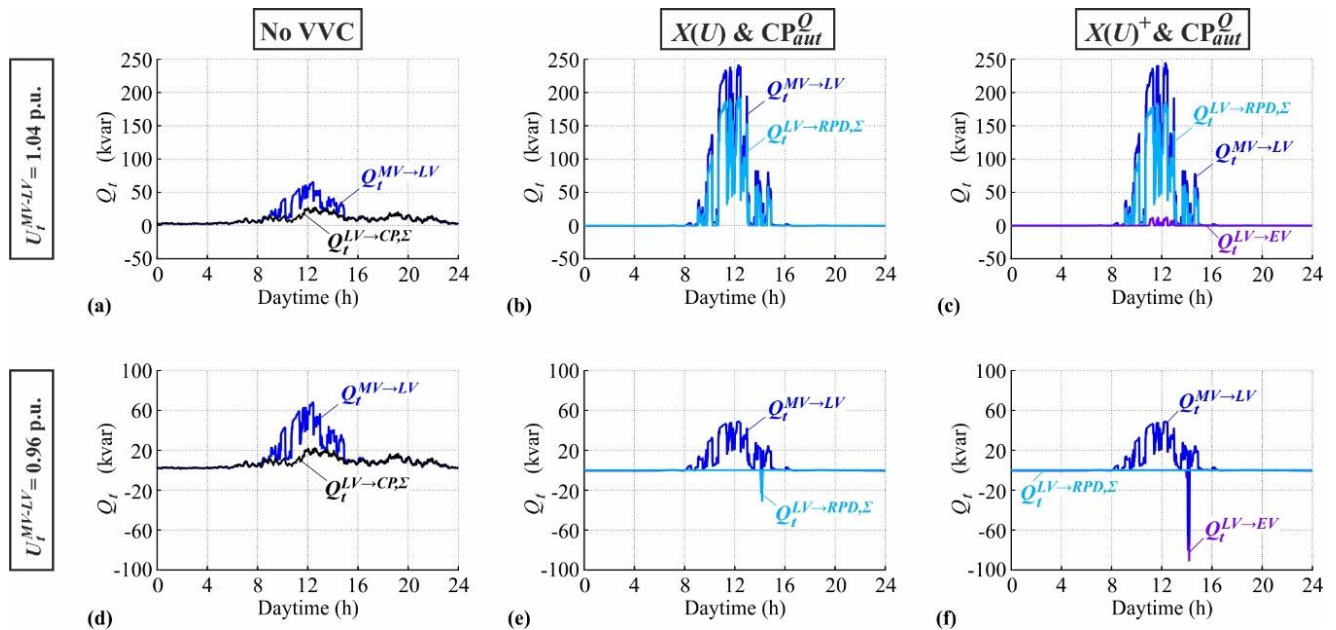


Fig. 6. Daily reactive power flows within the LV grid for different DTR primary voltages and VVC setups: (a) 1.04 p.u. without any VVC; (b) 1.04 p.u. with ' $X(U) & CP_{aut}^Q$ ' control; (c) 1.04 p.u. with ' $X(U)^+ & CP_{aut}^Q$ ' control; (d) 0.96 p.u. without any VVC; (e) 0.96 p.u. with ' $X(U) & CP_{aut}^Q$ ' control; (f) 0.96 p.u. with ' $X(U)^+ & CP_{aut}^Q$ ' control;

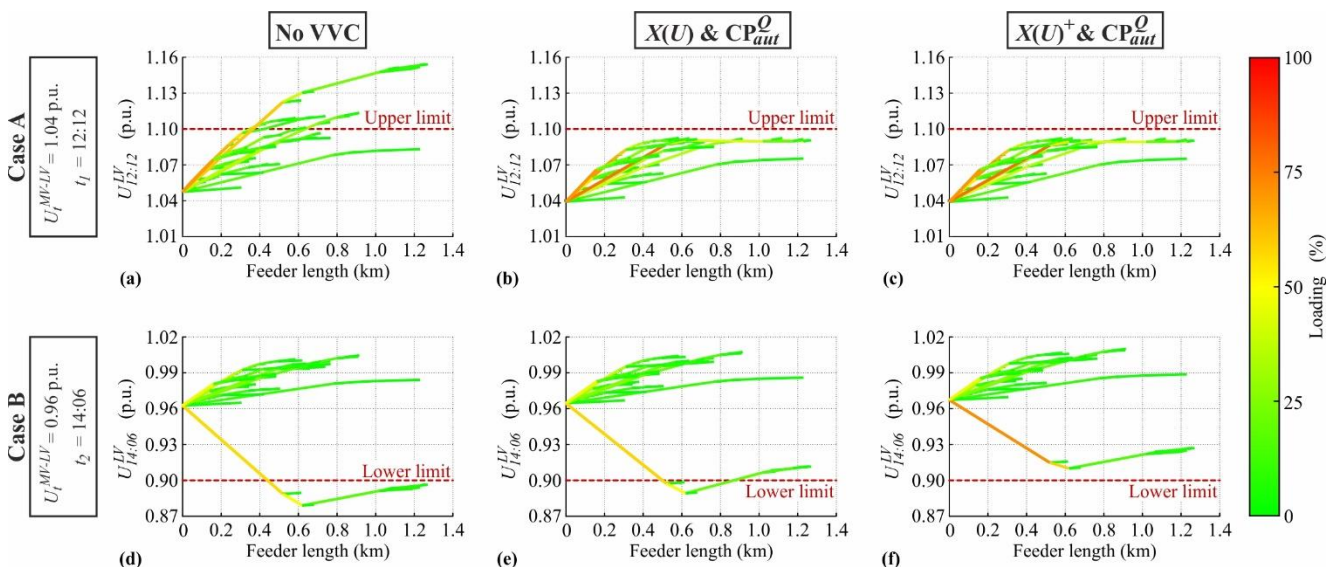


Fig. 7. LV grid state diagrams for different cases and control setups: (a) Case A without any VVC; (b) Case A with ' $X(U) & CP_{aut}^Q$ ' control; (c) Case A with ' $X(U)^+ & CP_{aut}^Q$ ' control; (d) Case B without any VVC; (e) Case B with ' $X(U) & CP_{aut}^Q$ ' control; (f) Case B with ' $X(U)^+ & CP_{aut}^Q$ ' control.

Grid state for critical cases

Fig. 7 shows the grid state diagrams for different cases and control setups. As shown in Fig. 7a and 7d, the voltage limits are drastically violated when no VVC is used: in case A, the upper limit is exceeded from a feeder length of 0.35 km, while in case B, the lower one is violated from 0.44 km feeder length. Maximum line segment loadings of 74.53 and 57.07 % occur in cases A and B, respectively.

Fig. 7b and 7e show that the ' $X(U)$ & CP_{aut}^Q ' control setup eliminates the upper but not the lower voltage limit violations: although the RPDs maintain acceptable voltages at the feeder's ends, the lower limit is violated in the middle part of the feeder in case B. However, compared to the setup without any VVC, the maximum line segment loading increases to 78.64 and 58.12 %, respectively, in cases A and B.

The ' $X(U)^+$ & CP_{aut}^Q ' control setup successfully eliminates all voltage limit violations, Fig. 7c and 7f. The maximum line segment loadings are increased to 78.67 and 72.01 % in cases A and B, respectively.

CONCLUSIONS

The investigated control setups differently affect the voltages, reactive power flows, and equipment loadings in low voltage grids. Combining $X(U)$ local control with CP_Q -Autarky may not maintain voltage limit compliance when bulk consumers such as electric vehicle parking garages are connected in the middle part of the low voltage feeders. The $X(U)^+$ local control setup guarantees voltage limit compliance in all conditions by incorporating reactive power provision of the bulk loads. Involving bulk loads in Volt/var control reduces the necessary rating of the $X(U)$ locally controlled reactive power devices but increases the uncontrolled reactive power exchanges between medium and low voltage grids and the equipment loading at the low voltage level.

Acknowledgments

This project was funded in the framework of the PED Programme, which is implemented by the Joint Programming Initiative Urban Europe and SET Plan Action 3.2., application number 37474305. The project is supported by the Austrian Ministry of Climate Action, Environment, Energy, Mobility, Innovation, and Technology (BMK), Technology Agency of the Czech Republic (TAČR) and Viable cities, a research program funded by the Swedish energy agency, Formas and Vinnova.

REFERENCES

[1] F. Katiraei and J.R. Agüero, 2011, "Solar PV Integration Challenges", *IEEE Power Energy Mag.* vol. 9, 62–71.
 [2] J. Gemassmer et al., 2021, "Challenges in Grid

Integration of Electric Vehicles in Urban and Rural Areas", *World Electr. Veh. J.* vol. 12, 206.
 [3] Q. Guo et al., 2019, "Review of Challenges and Research Opportunities for Voltage Control in Smart Grids", *IEEE Trans. Power Syst.* Vol. 34, 2790–2801.
 [4] M.H.J. Bollen and A. Sannino, 2005, "Voltage Control with Inverter-Based Distributed Generation", *IEEE Trans. Power Del.* vol. 20, 519–520.
 [5] E. Demirok et al., 2011, "Local Reactive Power Control Methods for Overvoltage Prevention of Distributed Solar Inverters in Low-Voltage Grids", *IEEE J. Photovolt.* vol. 1, 174–182.
 [6] D.-L. Schultis, A. Ilo, and C. Schirmer, 2019, "Overall Performance Evaluation of Reactive Power Control Strategies in Low Voltage Grids with High Prosumer Share", *Electr. Power Syst. Res.* vol. 168, 336–349.
 [7] A. Ilo and D.-L. Schultis, 2022, "A Holistic Solution for Smart Grids based on LINK-Paradigm: Architecture, Energy Systems Integration, Volt/var Chain Process", Springer International Publishing, Cham, Germany, 157–340.
 [8] A. Ilo and D.-L. Schultis, 2019, "Low-Voltage Grid Behaviour in the Presence of Concentrated Var-Sinks and Var-Compensated Customers", *Electr. Power Syst. Res.* vol. 171, 54–65.
 [9] D.-L. Schultis and A. Ilo, 2021, "Effect of Individual Volt/Var Control Strategies in LINK-Based Smart Grids with a High Photovoltaic Share", *Energies* vol. 14, 5641.
 [10] D.-L. Schultis, 2022, "Effective Volt/var Control for Low Voltage Grids with Bulk Loads", *Energies* vol. 15(5), 1950.
 [11] "Load Profile Generator", Available online: <https://www.loadprofilegenerator.de/> (accessed on 03 January 2022)
 [12] A. Bokhari et al., 2014, "Experimental Determination of the ZIP Coefficients for Modern Residential, Commercial, and Industrial Loads", *IEEE Trans. Power Del.* vol. 29, 1372–1381.
 [13] "CREST Demand Model", Available online: https://repository.lboro.ac.uk/articles/dataset/CREST_Demand_Model_v2_0/2001129/8 (accessed on 03 January 2022).
 [14] Y.-B. Wang et al., 2008, "Steady-State Model and Power Flow Analysis of Grid-Connected Photovoltaic Power System", *Proceedings IEEE International Conference on Industrial Technology*, 1–6.
 [15] A. Shukla, K. Verma, and R. Kumar, 2017, "Multi-Stage Voltage Dependent Load Modelling of Fast Charging Electric Vehicle", *Proceedings 6th International Conference on Computer Applications In Electrical Engineering-Recent Advances (CERA)*, 86–91.
 [16] D.-L. Schultis and A. Ilo, 2018, "TUWien_LV_TestGrids", *Mendeley Data*, v1, doi:10.17632/hgh8c99tnx.1.